

Catalysis Science & Technology

Accepted Manuscript



This is an *Accepted Manuscript*, which has been through the Royal Society of Chemistry peer review process and has been accepted for publication.

Accepted Manuscripts are published online shortly after acceptance, before technical editing, formatting and proof reading. Using this free service, authors can make their results available to the community, in citable form, before we publish the edited article. We will replace this *Accepted Manuscript* with the edited and formatted *Advance Article* as soon as it is available.

You can find more information about *Accepted Manuscripts* in the [Information for Authors](#).

Please note that technical editing may introduce minor changes to the text and/or graphics, which may alter content. The journal's standard [Terms & Conditions](#) and the [Ethical guidelines](#) still apply. In no event shall the Royal Society of Chemistry be held responsible for any errors or omissions in this *Accepted Manuscript* or any consequences arising from the use of any information it contains.

Cite this: DOI: 10.1039/c0xx00000x

www.rsc.org/xxxxxx

ARTICLE TYPE

Ionic liquid-functionalized graphene oxide as an efficient support for chiral salen Mn(III) complex in asymmetric epoxidation of unfunctionalized olefins

Weiguo Zheng,^a Rong Tan,^{*a} Shenfu Yin,^a Yaoyao Zhang,^a Guangwu Zhao,^a Yaju Chen,^a and Donghong Yin^{*a,b}

Received (in XXX, XXX) Xth XXXXXXXXX 20XX, Accepted Xth XXXXXXXXX 20XX

DOI: 10.1039/b000000x

Imidazolium-based ionic liquid (IL)-functionalized graphene oxide (GO) was prepared and used to support chiral salen Mn(III) complex. Technologies of characterization suggested that intact chiral complex was covalently appended on flat planes and edge of GO sheet through an imidazolium-based IL linker. The flexible layer-structure, as well as active role of IL linker in overall reaction, makes the novel heterogeneous catalyst efficient and universal in the enantioselective epoxidation of unfunctionalized olefins using NaClO as an oxidant. Remarkable enhancement of reaction rate with excellent conversion (99%) was observed over a wide range of alkenes either bulky or less (styrene, α -methylstyrene, indene, 1,2-dihydronaphthalene, 6-cyano-2,2-dimethylchromene, and 6-nitro-2,2-dimethylchromene). The enantiomeric excess (ee) for epoxides was also encouraging (in the range of 73–93%), except for styrene (ee, 40%) and α -methylstyrene (ee, 44%). More importantly, the catalyst was perfectly stable and could be reused for several times without significant loss of activity and enantioselectivity.

Introduction

Optically active epoxides are key intermediates in organic chemistry because they can undergo regioselective ring-opening reactions or functional group transformations, giving rise to a wide variety of biologically and pharmaceutically important compounds.^{1,2} Enantioselective epoxidation of olefins catalyzed by chiral salen Mn(III) complex is one of the most efficient strategies for obtaining enantiopure epoxides.^{3–10} Aqueous sodium hypochlorite (NaClO) used as an oxygen source has been drawn much attention in the transition, since it is reasonably stable, readily available, environment friendly and inexpensive. Despite of high yield and enantioselectivity of epoxides, long reaction time (3–24 h) is often required due to the limited mass transfer in the aqueous/organic biphasic system, resulting in relatively lower turnover frequency (TOF) value.^{5, 8, 11, 12} Chiral salen Mn(III) complexes with built-in phase-transfer capability have been developed for the biphasic condition.^{13, 14} Recently, we have

prepared this type of complexes by covalent linkage of polyether chains-modified limidazolium IL moieties with chiral salen ligand at two sides of 5,5'-positions.¹⁵ Remarkable enhancement of reaction rate was observed over the catalysts in the water-dichloromethane biphasic system due to the inherent phase-transfer capacity originated from polyether chain. More importantly, limidazolium-based IL moiety with special 'ionophilicity' and polarity played positive effect on stabilizing the chiral salen Mn(III) complex and preventing the degradation of catalyst during the epoxidation with NaClO. Unfortunately, the homogeneous complexes were difficult to separate from the reaction system. Inevitable leaching loss of catalyst resulted in gradual decrease in activity during reuse. An ideal solution to this problem is attaching the homogeneous phase-transfer catalyst to an insoluble support, so that the catalysts can be easily separated from the reaction mixture by simple filtration or centrifugation.

Recently, layered multifunctional materials, such as zinc phosphonate-phosphate¹⁶ or layered double hydroxides (LDHs),^{17, 18} have drawn considerable attention in the field of heterogeneous catalysis due to the tailorable interlayer spaces. Apart from facilitating separation, location of catalytic sites in the flexible interlayer regions renders all active centres accessible to reactants during the reaction, which in turn allows the heterogeneous catalytic reactions to be carried out under pseudo-homogeneous conditions. GO, a new layered material, has attracted increasing attention for the scientists all over the world.^{19–21} The ultrahigh specific surface area (theoretical 2630 m² g⁻¹), especially the unique surface properties (multiple oxygenated functional groups on the basal planes and edge), provides GO sheet with a great

^a Institute of Fine Catalysis and Synthesis, Key Laboratory of Chemical Biology and Traditional Chinese Medicine Research (Ministry of Education), Hunan Normal University, Changsha, Hunan, 410081, China;

^b Technology Center, China Tobacco Hunan Industrial Corporation, NO. 426 Laodong Road, Changsha, Hunan, 410014, China.

Fax: +86-731-8872531; Tel: +86-731-8872576; E-mail: yiyangtanrong@126.com (R. Tan) or yindh@hunnu.edu.cn (D. Yin)

capability for loading catalytically active molecules through covalent or non-covalent methods.²²⁻²⁴ Lately, we have intercalated the Mn²⁺ ions into the layered GO sheets through coordination of Mn²⁺ ions with the oxygenated functional groups of GO sheet.²⁵ The layered GO sheet with flexible interlayer spaces indeed favoured reagents' diffusion towards catalytic active sites, resulting in high efficiency and good universality of the heterogeneous Mn²⁺/GO nanocomposite in the epoxidation of alkenes with aqueous H₂O₂. The promising initial work encouraged us to employ the GO sheet as an efficient support for chiral salen Mn(III) complex to provide an efficient and reusable catalyst for the asymmetric epoxidation of olefins with aqueous NaClO. Considering the positive effect of imidazolium-based IL on stabilizing and activating chiral salen Mn(III) complex, we thus decided to utilize an imidazolium-based IL linker to covalently attach the chiral salen Mn(III) complex to GO sheet. The IL linker with specific miscibility was also expected to fine tune the surface properties of the GO sheet, improving compatibility of the heterogeneous catalyst in the aqueous/organic biphasic reaction.

Herein, imidazole-modified GO sheet was synthesized and used to immobilize the chiral salen Mn(III) complex through the N-alkylation of imidazole groups on GO sheet with the methyl chloride group (-CH₂Cl) at 5 position of chiral salen ligand. Chiral salen Mn(III) complex was thus appended covalently on the flat planes and edge of GO sheet through an imidazolium-based IL linker. It has proved that the novel catalyst was efficient and universal in the enantioselective epoxidation of unfunctionalized olefins with NaClO. Remarkable enhancement of reaction rate with high TOF values was observed over a wide range of alkenes either bulky or less. Furthermore, the heterogeneous catalyst can be quantitatively recovered from the reaction mixture by centrifugation for steady reuse. Thus, the problems associated with the mass transfer and separation of catalyst in aqueous/organic biphasic reactions can be well solved.

Experimental

Materials and reagents

(±)-1,2-diaminocyclohexane and high-purity graphite (99.9999%, 200 mesh) were purchased from Alfa Aesar. Indene and 1,2-dihydronaphthalene were obtained by TCI. Pyridine-N-oxide (PyNO) was bought from Aldrich. Other commercially available chemicals were laboratory grade reagents from local suppliers. All of the solvents were purified by standard procedures.²⁶ Styrene and indene were passed through a pad of neutral alumina before use. 6-cyano-2,2-dimethylchromene and 6-nitro-2,2-dimethylchromene were synthesized according to the literature procedures.²⁷ GO was prepared by the oxidation of high-purity graphite powder with H₂SO₄/KMnO₄ according to the method of Hummers and Offeman.²⁸ 3-tert-Butyl-5-chloromethyl-2-hydroxybenzaldehyde were prepared according to the described procedures.²⁹ [(R,R')-(N,N'-bis(3,5-di-tert-butylsalicylidene)-1,2-cyclohexanediaminato)] manganese(III) chloride (denoted as neat complex, as shown in Fig. 1) was prepared according to the described procedures.³

Methods

Surface structure of the samples was measured using a

Shimadzu SEM (Superscan SSX-550, Japan). X-ray diffraction (XRD) patterns were recorded on a Philips X'PERT-Pro-MPD diffractometer using Cu K α radiation ($\lambda = 1.542 \text{ \AA}$). A continuous scan mode was used to collect the 2θ from 5° to 80° . Fourier transform infrared (FT-IR) spectra were obtained as potassium bromide pellets with a resolution of 4 cm^{-1} and 32 scans in the range $400\text{--}4000 \text{ cm}^{-1}$ using an AVATAR 370 Thermo Nicolet spectrophotometer. X-ray Photoelectron Spectroscopy (XPS) data were obtained with an ESCALab220i-XL electron spectrometer from VG Scientific using $300 \text{ W Al K}\alpha$ radiation. The base pressure was about $3 \times 10^{-7} \text{ Pa}$. Ultraviolet-visible light (UV-vis) spectra were recorded on a UV-vis Agilent 8453 spectrophotometer. The samples were fully dispersed in dichloromethane under sonication. The suspension was poured into a 1 cm quartz cell for UV-vis absorption with dichloromethane as the reference. Thermogravimetric and differential thermogravimetric (TG-DTG) curves were obtained on a NETZSCH STA 449C thermal analyzer. Samples (*ca.* 0.01 g) were heated from room temperature up to 900°C with 10 K/min under air flow using alumina sample holders. Elemental analyses were carried out on Vario EL III Elemental analyses made in Germany. ¹H NMR spectra of samples were recorded on a Varian-500 spectrometer with TMS as an internal standard. Thin layer chromatography (TLC) was conducted on glass plates coated with silica gel GF₂₅₄. Mn ion content was measured by the method of complexometry with ethylenediamine tetraacetic acid (EDTA).³⁰ The conversion and ee values were measured by a 6890N gas chromatograph (Agilent Co.) equipped with a chiral capillary column (HP19091G-B213, $30 \text{ m} \times 0.32 \text{ mm} \times 0.25 \text{ }\mu\text{m}$).

Preparation of asymmetric chiral salen Mn(III) complex

Asymmetric chiral salen Mn(III) complex of (R,R)-N-(3,5-di-tert-butylsalicylidene)-N'-[3-tert-butyl-5-chloromethylsalicylidene]-1,2-cyclohexanediaminato] manganese(III) chloride (as shown in Chart 1) was synthesized as described earlier.³¹

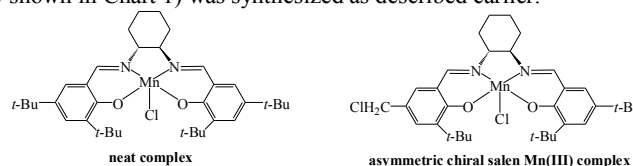


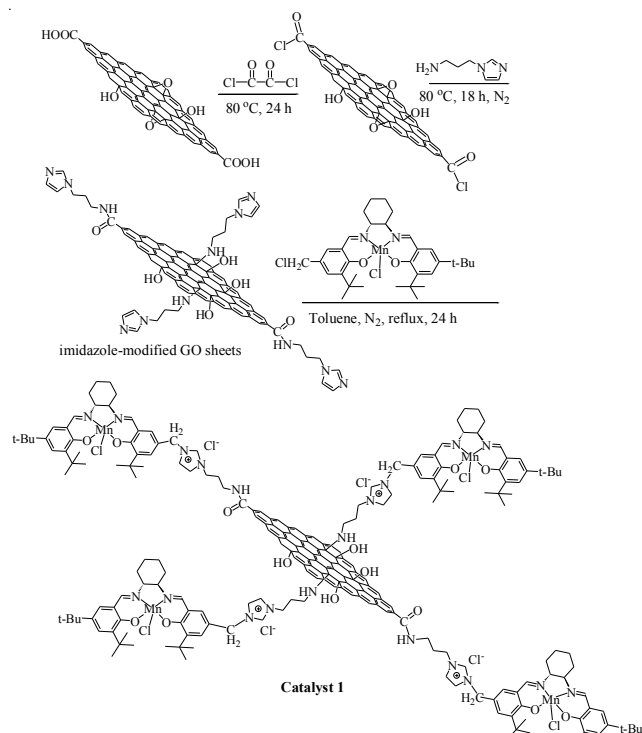
Chart 1 The structures of neat and asymmetric chiral salen Mn(III) complexes.

Preparation of catalyst 1

The preparation of IL-functionalized GO supported chiral salen Mn(III) complex (denoted as **catalyst 1**) was outlined in Scheme 1.

Synthesis of imidazole-modified GO sheet: GO (0.25 g) was stirred in oxalyl chloride (100 mL) at 80°C for 24 h to activate the carboxylic units by forming the corresponding acyl chlorides. After removing excess oxalyl chloride, the mixture was washed with anhydrous THF and dried at room temperature under vacuum to afford the acyl chlorinated GO as a brown solid. The acyl chlorinated GO (0.15 g) was treated with 1-(3-aminopropyl)imidazole (50 mL) at 80°C for 18 h under N_2 . The reaction mixture was filtrated through $0.2 \text{ }\mu\text{m}$ PTFE filter. The solid residue was then washed with dichloromethane and diethyl

ether to remove the unreacted 1-(3-aminopropyl)imidazole. The imidazole-modified GO sheets were obtained as light brown solid. FT-IR (KBr): $\nu_{\text{max}}/\text{cm}^{-1}$ 3329, 2881, 1658, 1556, 1224, 1110, 873, 747, 662, 620. The imidazole content in the modified GO sheet is 0.56 mmol/g, which was determined according to the content of nitrogen element analyzed by elemental analyses.



Scheme 1 Synthesis of catalyst 1.

Synthesis of catalyst 1: The imidazole-modified GO sheet (0.5 g) was mixed with the asymmetric chiral salen Mn(III) complex (0.63 g, 1 mmol) in toluene (100 mL). After refluxing for 24 h under nitrogen protection, the black slurry was filtrated and washed with dry toluene and diethyl ether. The obtained solid was extracted thoroughly in dichloromethane using a Soxlet apparatus, and then dried under vacuum at room temperature to give the **catalyst 1**. FT-IR (KBr): $\nu_{\text{max}}/\text{cm}^{-1}$ 3330, 2950, 2910, 2861, 1658, 1614, 1556, 1224, 1110, 837, 746, 660, 619, 571, 418; UV-vis (CH_2Cl_2): $\lambda_{\text{max}}/\text{nm}$ 322, 401, 498; Mn ion content: 0.47 mmol/g.

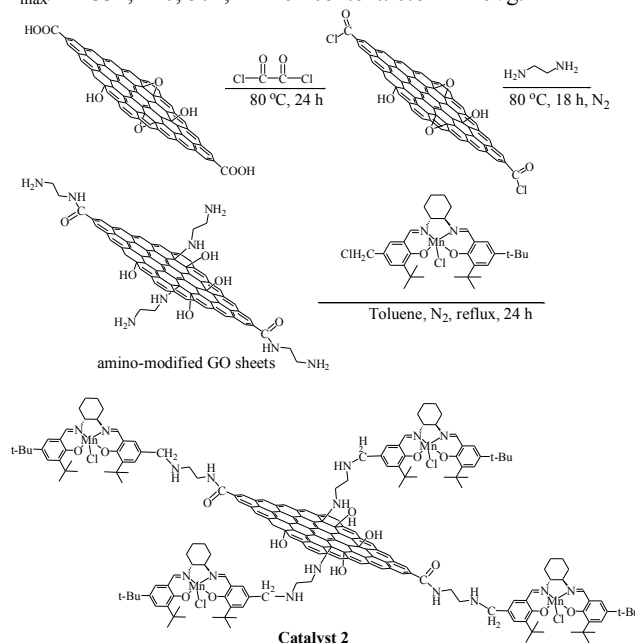
Preparation of catalyst 2

For comparison, the catalyst of IL-free counterpart (denoted as the **catalyst 2**), in which chiral salen Mn(III) complex was directly anchored to the flat planes and edge of GO sheet through an alkyl linker, was also prepared according to process outlined in Scheme 2.

Synthesis of amino-modified GO sheet: Acyl chlorinated GO sheet (0.15 g) were dispersed in ethylenediamine (50 mL) at 80 °C for 18 h under N_2 . The obtained slurry was filtrated through 0.2 μm PTFE filter, and then successively washed with dichloromethane (5 \times 20 mL) and diethyl ether (5 \times 20 mL) to remove the unreacted ethylenediamine. The residue was dried at room temperature under vacuum to give the amino-modified GO

sheets as brown solid. FT-IR (KBr): $\nu_{\text{max}}/\text{cm}^{-1}$ 3430, 3162, 2920, 2810, 2363, 1650, 1556, 1224, 1151, 1110, 960, 871, 588, 457. The content of amino group in the modified GO sheet is 0.73 mmol/g, which was determined according to the content of nitrogen element analyzed by elemental analyses.

Synthesis of catalyst 2: The amino-modified GO sheet (0.5 g) was added to a solution of the asymmetric chiral salen Mn(III) complex (0.63 g, 1 mmol) in dry toluene (100 mL). The resulting suspension was refluxed for 24 h under nitrogen protection. After being filtrated and washed with dry toluene and diethyl ether, the black crude product was extracted thoroughly in dichloromethane using a Soxlet apparatus. The residue was dried at room temperature under vacuum for 24 h to give the **catalyst 2**. FT-IR (KBr): $\nu_{\text{max}}/\text{cm}^{-1}$ 3430, 3266, 3008, 2951, 2867, 1658, 1610, 1524, 1389, 1224, 1164, 1036, 985, 569, 417; UV-vis (CH_2Cl_2): $\lambda_{\text{max}}/\text{nm}$ 331, 420, 502; Mn ion content: 0.61 mmol/g.



Scheme 2 Synthesis of catalyst 2.

Preparation of IL-complex

The other control catalyst of GO-free counterpart (denoted as **IL-complex**), in which imidazolium-based IL was covalently bonded on chiral salen Mn(III) complex at 5-position, was also prepared through N-alkylation of 1-methylimidazole with the benzyl chloride group ($-\text{CH}_2\text{Cl}$) of asymmetric chiral salen Mn(III) complex. The structure of **IL-complex** was shown in Chart 2.

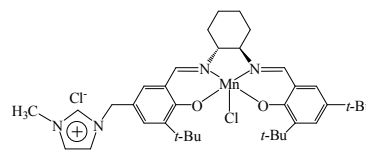


Chart 2 The structures of **IL-complex**.

Catalyst testing

The selected catalyst (4 mol% on substrate, based on Mn content in catalyst), unfunctionalized alkene (1 mmol) and PyNO (2 mmol, 0.19 g) were added into dichloromethane (2 mL) under

stirring at 0 °C. Buffered NaClO as an oxidant (2 mmol, pH=11.5) was then added in four equal portions. The progress of the epoxidation reaction was monitored by gas chromatography. After the reaction, the heterogeneous catalyst was recovered by centrifugation, washed with dichloromethane, and successively reused for subsequent epoxidation. The reaction solution was separated by separatory funnel. The aqueous phase was extracted with dichloromethane for several times. The extract was combined with organic phase, and dried over anhydrous sodium sulfate. Further purification of the dichloromethane phase by flash column chromatography afforded the epoxides. The conversion and ee value were measured by a 6890N gas chromatograph (Agilent Co.) equipped with the chiral capillary column (HP19091G-B213, 30 m×0.32 mm×0.25 µm) and the FID detector. Nitrogen was used as the carrier gas with a flow of 30 mL min⁻¹. The retention times of the corresponding chiral epoxides are as follows: (a) styrene epoxide: the column temperature is 90 °C, t_R =15.2 min, t_S =15.7 min; (b) α -methylstyrene epoxide: the column temperature is 80 °C, t_S =16.3 min, t_R =16.5 min; (c) indene epoxide: the column temperature was programmed from 80 to 180 °C with 8 °C min⁻¹, t_{SR} =11.5 min, t_{RS} =11.9 min; (d) 1,2-dihydronaphthalene epoxide: the column temperature was programmed from 80 to 180 °C with 6 °C min⁻¹, t_{SR} =13.4 min, t_{RS} =13.6 min; (e) 6-cyano-2,2'-dimethylchromene epoxide: the column temperature was programmed from 80 to 200 °C with 4 °C min⁻¹, t_{SS} =24.0 min, t_{RR} =24.3 min; (f) 6-nitro-2,2'-dimethylchromene epoxide: the column temperature was programmed from 80 to 200 °C with 4 °C min⁻¹ and retained at 200 °C for 5 min, t_{SS} =30.3 min, t_{RR} =30.8 min.

Results and discussion

Preparation and characterization of catalysts

GO with unique layered structure, as well as the ultrahigh specific surface area, is an excellent candidate for catalyst support. In particular, the abundant reactive oxygen functional groups on the surface provide GO sheet with large capability of loading catalytic molecules through covalent or non-covalent approaches. In general, GO sheet requires further modification to confer high dispersion in a range of media for catalytic reactions.^{32, 33} ILs, as modifiers in support systems, can fine tune the surface properties of support and transfer the properties of ILs to materials,^{34, 35} which are expected to improve the compatibility of the heterogeneous catalyst in aqueous/organic biphasic reaction. Furthermore, ILs derived from N,N-dialkylimidazolium were found to activate and stabilize the chiral salen Mn(III) complex during the process of the epoxidation.^{36, 37} Thus, we decided to covalently immobilize chiral salen Mn(III) complex on imidazolium-based IL-functionalized GO sheet to produce an efficient and reusable catalyst for asymmetric epoxidation of unfunctionalized alkenes with NaClO. Given that single point attachment fashion with a flexible spacer group minimizes local steric restriction arisen from support,³⁸ a strategy that we designed here is to covalently append chiral salen Mn(III) complex onto GO sheet through an imidazolium-based IL linker at 5-position of salen unit.

The preparation of **catalyst 1** is shown in Scheme 1. The layered

GO sheet was activated upon treatment with oxalyl chloride and further reacted with an excess of 1-(3-aminopropyl)imidazole to conjugate imidazole units at the edge of GO sheet through amide bond (O=C-N). Moreover, the chemically reactive epoxy groups on the basal planes of GO can also undergo nucleophilic ring-opening reaction with the attack of amine group in 1-(3-aminopropyl)imidazole. N-alkylimidazole group was thus decorating the edge and flat planes of GO sheet, forming the imidazole-modified GO sheet. Successive N-alkylation of the N-alkylimidazole group on GO sheet with the benzyl chloride group (-CH₂Cl) at 5-position of asymmetric chiral salen Mn(III) complex resulted in the covalently appending chiral salen Mn(III) complex on the edge and basal planes of GO sheet through imidazolium-based IL linker. Removal of the unanchored homogeneous species by Soxhlet extraction gave **catalyst 1** as black powder.

For comparison, the IL-free counterpart of **catalyst 2**, in which chiral salen Mn(III) complex was directly anchored to GO sheet through alkyl linker, was also prepared according to a modified preparation procedure.³¹ The synthesis route was outlined in Scheme 2. During the procedure, ethylenediamine was used to modify the surface of GO sheet through the amidation of carboxylic acid group and nucleophilic ring-opening reaction of epoxy group. The decorative amino groups (-NH₂) located at the edge and flat planes of GO sheet were readily alkylated with the benzyl chloride group (-CH₂Cl) at 5-position of asymmetric chiral salen Mn(III) complex, resulting in covalently appending chiral salen Mn(III) complex on GO sheet through alkyl chain. Removal of the unanchored homogeneous species by Soxhlet extraction gave **catalyst 2** as black powder.

Interestingly, **catalyst 1** exhibits better dispersion than the IL-free counterpart of **catalyst 2** in both water (Fig. 1A) and dichloromethane (Fig. 1B). Stable suspension is observed over the **catalyst 1** (Fig. 1A-b and Fig. 1B-b), suggesting better compatibility of heterogeneous **catalyst 1** in the aqueous/organic biphasic reaction. We thus suspected that high dispersion was related to the special solubility of the imidazolium-based IL modifier. The high dispersion of **catalyst 1** with easy accessibility of active sites enables the heterogeneous catalyst to behave as pseudo-homogeneous catalyst in aqueous/organic biphasic reaction.

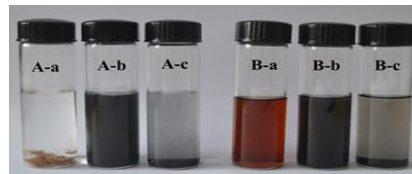


Fig. 1 Photographs of neat complex (a), **catalyst 1** (b) and **catalyst 2** (c) in water (A) and in dichloromethane (B).

Characterization of Samples

XRD

XRD patterns are used to study the change of GO in structure during the loading process. Fig. 2 shows powder XRD patterns of pristine GO material, catalysts **1** and **2**. GO displays a strong (002) peak centered at 10.5°, suggesting the layered structure with an average interlayer distances of ca. 0.85 nm (Fig. 2a). While, the sharp diffraction peak disappears, accompanied by the

appearance of a new weak peak at $2\theta = 25.98^\circ$, after the introduction of bulky imidazolium IL-tagged chiral salen Mn(III) complex moiety (Fig. 2b). A reasonable explanation for these observations might be that regularly aggregated GO sheet are exfoliated to single or fewer layer during the modification.³⁹ It is well known that individual GO platelets are interlinked via a network of hydrogen bonds mediated by oxygen-containing functional groups, as well as the van der Waals forces between layers.⁴⁰ Intercalation of bulky imidazolium IL-tagged chiral complex into the interlayer spacing may weaken the interlinked driven forces between GO layers, enabling facile exfoliation of the layered GO material. Delamination of the nanosheet is also observed in **catalyst 2**, since it displays the XRD pattern similar to **catalyst 1** (Fig. 2c vs b). The featured structure of exfoliated nanosheet makes all active sites accessible, which thus allows the heterogeneous catalyst to behave as pseudo-homogeneous catalyst in the reaction.

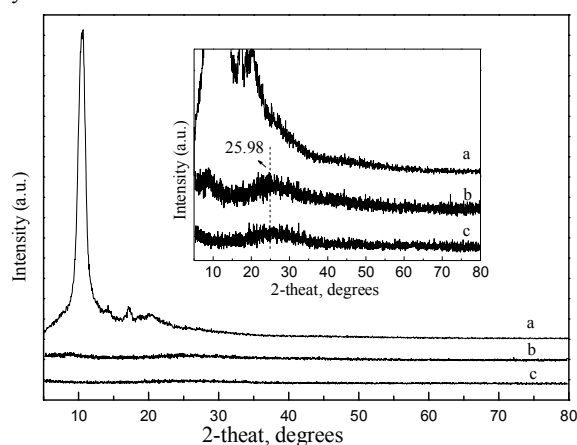


Fig. 2 XRD patterns of GO (a), **catalyst 1** (b) and **catalyst 2** (c) (The inset is the magnified XRD patterns of GO (a), **catalyst 1** (b) and **catalyst 2** (c)).

SEM

SEM images provide direct information on microstructure and morphology of pristine GO sheet, catalysts **1** and **2**, as shown in Fig. 3. Obviously, pure GO support has a typical layered structure in the SEM image (Fig. 3A). GO nanosheets agglomerate with each other through a network of hydrogen bonds and van der Waals forces between layers.⁴⁰ While, the interlayer interactions of GO nanosheets are disturbed by the introduction of IL-tagged chiral salen Mn(III) complex moiety. Exfoliated or at least loosened lamellar structure is observed in the SEM image of **catalyst 1**, as shown in Fig. 3B. It is logical to deduce that the IL-tagged chiral salen Mn(III) complex are not only decorating the edge of GO sheet, but also intercalated into the interlayer spacing. Bulky organometallic moieties on the flat planes of GO sheet prevent the restacking of the nanosheet, thus providing accessible void for reagents. **Catalyst 2**, in which chiral salen Mn(III) complex is direct anchored on the surface of GO sheet through a alkyl chain, also exhibits intercalated and exfoliated morphology in SEM image (Fig. 3C). Notably, the basal nanosheet of GO support is intact in catalysts **1** and **2**. It means that chemically reactive oxygen moieties provide the anchoring sites for the

organometallic moieties, and GO sheet backbone doesn't take part in the grafting.

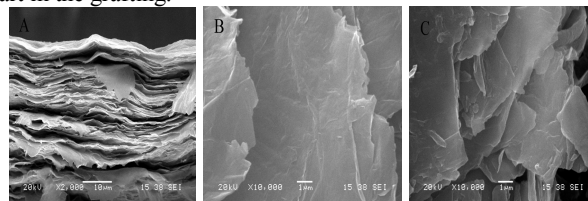


Fig. 3 SEM images of GO (A), **catalyst 1** (B) and **catalyst 2** (C).

FT-IR

The anchoring behavior of chiral salen Mn(III) complex on GO sheet was investigated by FT-IR analysis in detail. Fig. 4 shows the FT-IR spectra of catalysts **1** and **2**, as well as pristine GO sheet and neat chiral salen Mn(III) complex for comparison. Pristine GO shows the skeletal vibrations of non oxidized graphitic domains at 1621 cm^{-1} ,^{41,42} as well as the characteristic vibration bands of oxygen-containing groups at round 3300 , 1735 , 1224 , and 1050 cm^{-1} in the FT-IR spectrum, which are associated with the stretching vibration modes of COO-H/O-H, carboxylic C=O, C-OH, and epoxy C-O groups presented on the surface of GO, respectively (Fig. 4a).^{24,43,44} Treatment of pristine GO with 1-(3-aminopropyl)imidazole results in the changes of carboxylic and epoxy groups, as shown in the FT-IR spectrum of imidazole-modified GO (Fig. 4b). After imidazole modification, the band corresponding to carboxylic C=O group disappears with the formation of a new band at 1658 cm^{-1} , which is the characteristic stretching vibration of C=O in amide (-CONH-) group (Fig. 4b vs a). It provides a convincing proof that 1-(3-aminopropyl)imidazole moiety gets anchored on the edge of the GO sheet through an amidation process. Furthermore, the characteristic band at 1050 cm^{-1} , assigned to the C-O stretching vibration of the epoxy group, also almost disappears in the FT-IR spectrum of imidazole-modified GO. This could be interpreted as evidence that epoxy groups interact with amine groups during the modification. Actually, amine group in 1-(3-aminopropyl)imidazole can induce the nucleophilic ring-opening reaction of epoxide,^{45,46} which makes the successful functionalization of N-alkyl imidazole groups on the flat planes of GO sheet. Additional new characteristic bands at 1556 and 1110 cm^{-1} associated with the ring stretching of imidazole moiety⁴⁷ further confirm the presence of imidazole moiety on the planes and edge of GO sheet (Fig. 4b). It is imidazole modifier that is responsible for the covalent anchoring chiral salen Mn(III) complex on GO sheet by forming an imidazolium-based IL linker, as shown in Scheme 1. Grafting the complex onto the imidazole-modified GO sheet gives new characteristic bands at around 1614 , 571 and 418 cm^{-1} , which are assigned to the stretching vibrations of C=N, Mn-O and Mn-N in the chiral salen Mn(III) framework (Fig. 4c).¹⁵ Obviously, the structure of the complex is maintained in the immobilized state. Notably, the characteristic vibrations of C=N, Mn-O and Mn-N slightly shift from 1608 , 565 and 416 cm^{-1} to 1614 , 571 and 418 cm^{-1} , respectively, after grafting, compared with those of the neat complex (Fig. 4c vs e). The observations indicate that chiral salen Mn(III) complex is covalently anchored on GO sheet through the imidazolium-based

IL linker. Election-deficient effect of the imidazolium cation results in red shift of the characteristic bands.^{15,48}

The FT-IR spectrum of **catalyst 2** is similar to that of **catalyst 1** (Fig. 4d vs. c), except for the absence of the characteristic stretching vibration of imidazole ring (at 1556 and 1110 cm^{-1}). The difference is related to the absence of imidazolium-based IL moiety in the framework of **catalyst 2**. Furthermore, the characteristic band derived from the stretching vibration mode of C=O in –CONH– group (at around 1658 cm^{-1}) in the FT-IR spectrum of **catalyst 2** provides an evidence that chiral salen Mn(III) complex is directly anchored onto amino-functionalized GO sheet by forming amide group (Fig. 4d), as shown in Scheme 2. Notably, compared with **catalyst 2**, a significant feature observed for **catalyst 1** is the presence of imidazolium-based IL linker that positively affects catalytic performance of **catalyst 1** in the aqueous/organic biphasic epoxidation.

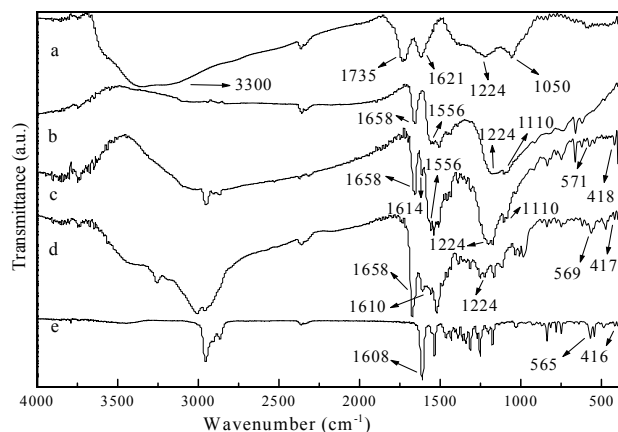


Fig. 4 FT-IR spectra of pristine GO sheet (a), imidazole-modified GO (b), **catalyst 1** (c), **catalyst 2** (d) and neat complex (e).

XPS

XPS was employed to gain further insights into surface chemical changes associated with the reaction shown in Scheme 1 and 2. Fig. 5 shows the XPS of pristine GO, imidazole-modified GO sheet and amino-modified GO sheet. As expected, only C1s and O1s peaks are seen in the XPS survey spectrum for pristine GO (Fig. 5a). A new N1s (399.5 eV) peak appears, accompanied by the reduced O1s peak with respect to the C1s peak, in the XPS survey spectrum of imidazole-modified GO sheet (Fig. 5a). It suggests that GO was modified by imidazole group through reaction with oxygenated functional groups. The deduction also can be drawn from the high-resolution C1s XPS spectra of GO and imidazole-modified GO sheet (Fig. 5b). Four typical peaks associated with C-C/C=C (284.6 eV), C-OH (285.7 eV), C-O-C (286.7 eV) and O=C-O (289.4 eV) groups are obvious in the high-resolution C1s XPS spectra of GO.⁴⁹ Deconvolution of the peak area evaluates the amount of oxygenated functional groups on GO sheets. It shows that there are 12% of the carbon atoms associated with C-OH, 58.5% associated with C-O-C, and 20.5% associated with O=C-O on pristine GO. While, the O=C-O peak for GO weakens obviously (from 20.5% to 7%) upon the imidazole modification. The reduction of O=C-O group together with the newly formed peaks associated with O=C-N (287.8 eV, 7.5%) and C-N (285.4 eV)⁴⁹ in C1s XPS spectrum of imidazole-modified GO sheet indicates

the amidation process at edge of GO. Furthermore, the modification also results in a significant decrease in the intensity of C-O-C peak (from 58.5% to 16.5%) accompanied by the increase of C-OH group (from 12% to 68%). It demonstrates the nucleophilic ring-opening reaction of epoxide group with the amino group in 1-(3-aminopropyl)imidazole during the modification. The results indicate that the edge and flat planes of GO sheet are modified by N-alkylimidazole.

Amino-modified GO shows similar tendency in the XPS survey (Fig. 5a) and high-resolution C1s spectra (Fig. 5b), as compared with imidazole-modified GO sheet. It confirms the successful modification of N-alkyl chain on the edge and flat planes of the GO sheet through an amidation process and nucleophilic ring-opening reaction, respectively, as shown in Scheme 2. Furthermore, we noticed that an additional Cl 2p peak at 198.8 eV⁵⁰ is obvious in the XPS survey spectrum of amino-modified GO. The Cl 2p peak should be probably due to that the hydrogen chloride arisen from amidation process was captured by terminal amino groups on GO sheet. It provides an indirect evidence for the presence of terminal amino groups on GO sheet, as well as the modification through an amidation process.

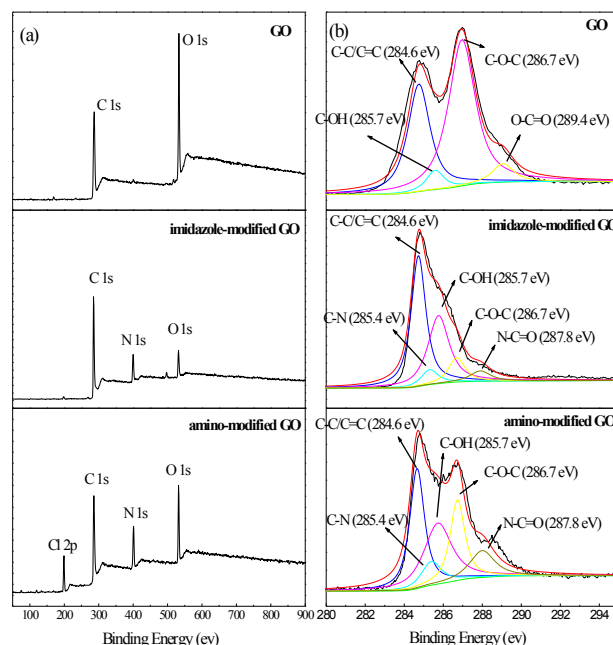


Fig. 5 XPS survey spectra of GO sheet, imidazole-modified GO and amino-modified GO (a) and C1s XPS spectra of GO sheet, imidazole-modified GO and amino-modified GO (b).

UV-vis

Fig. 6 shows UV-vis spectra of catalysts **1**, **2** and neat chiral salen Mn(III) complex. It gives more obvious evidence for the successful grafting, since the characteristic peaks of neat complex at around 433 and 506 nm show blue shifts after the complex being grafted. The peak at 433 nm is due to the charge-transfer transition from metal to salen ligand, and the peak at 506 nm is attributed to *d-d* transition of complex.¹⁵ As for **catalyst 1**, the characteristic peaks associated with metal-to-ligand charge-transfer transition and *d-d* transition of complex are significant shifted to 401 and 498 nm, respectively (Fig. 6b vs a). The behaviour is mainly attributed to the election-deficient effect of

imidazolium cation at 5-position of the chiral salen ligand in the framework of **catalyst 1**. Blue shifts of the characteristic peaks from 433 and 506 nm to 420 and 502 nm, respectively (Fig. 6c vs a), are also observed in the UV-vis spectrum of **catalyst 2**, indicating the covalently grafting chiral salen Mn(III) complex on amino-modified GO sheet.⁵¹

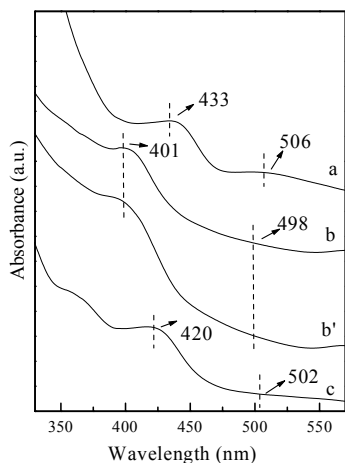


Fig. 6 UV-vis spectra of neat complex (a), **catalyst 1** (b), the recovered **catalyst 1** after the 7th reuse (b'), and **catalyst 2** (c).

Thermal analysis

Thermal analysis had been used to monitor the decomposition profiles of **catalyst 1**, as well as the neat complex and pristine GO sheet for comparison. The results obtained are depicted in Fig. 7.

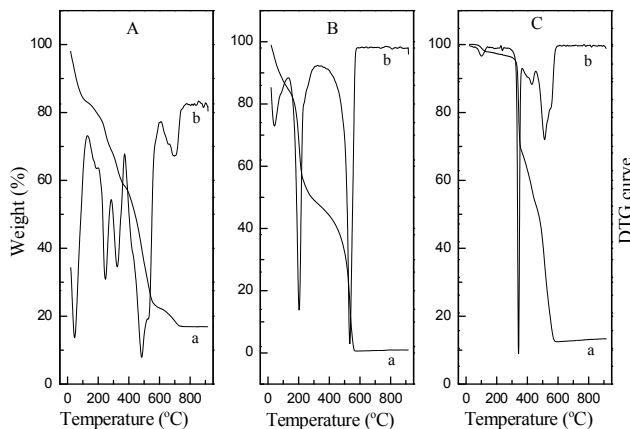


Fig. 7 TG-DTG curves of **catalyst 1** (A), pristine GO sheet (B) and neat complex (C) ((a) thermogravimetric curves; (b) differential thermogravimetric curves).

Catalyst 1 shows five distinct steps of weight losses in combined TG-DTG curves upon heating from room temperature to 900 °C under airflow (Fig. 7A). The first weight loss at 90 °C is due to the removal of surface-adsorbed water. The second weight loss at 249 °C (ca. 9.1%) accounts for the pyrolysis of oxygenated functional groups on the GO surface.⁴⁹ Interestingly, the decomposition temperature of the oxygen functional groups in **catalyst 1** increases compared with that of pristine GO sheet (at 200 °C) (Fig. 7A vs. B), suggesting the mutual stabilization of GO sheet and the IL moieties. The third weight loss at 325 °C (ca.

15%) is assigned to the cleavage of the *tert*-butyl groups in salen ligand, since neat complex shows the similar major weight loss in the temperature range (Fig. 7A vs. C). Successive pyrolysis of the remaining ligand moiety occurs in the range of 368–596 °C, which is overlapped with the oxidative decomposition of the GO residue, giving a major weight loss (ca. 32%). The last weight loss at 702 °C (ca. 6.6%), which is absent in the combined TG-DTG curves of neat complex and pristine GO sheet (Fig. 7A vs. B and C), is logical to assign to the complete decomposition of imidazolium IL moiety. The decomposition extends up to ca. 761 °C, leaving non-removable residue (ca. 17%) belonged to the formation of manganese oxide in air at high temperature. The results provide an indirect proof for the covalent linkage of chiral salen Mn(III) complex on GO sheet through an imidazolium-based IL linker.

Catalytic performances

Although heterogeneous, IL-tagged **catalyst 1** shows good compatibility in both aqueous and organic solvents. We thus proposed that the heterogeneous **catalyst 1** should behave as a pseudo-homogeneous catalyst in aqueous/organic biphasic system. The catalytic performance of **catalyst 1** in the enantioselective epoxidation of different substrates at 0 °C, using aqueous NaClO as oxygen source in dichloromethane, are summarised in Table 1.

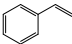
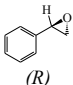
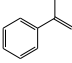
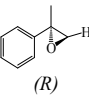
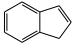
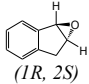
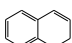
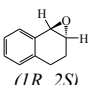
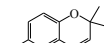
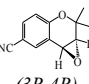
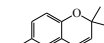
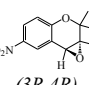
Notably, the IL-tagged **catalyst 1** significantly accelerated the aqueous/organic biphasic epoxidation. Using aqueous NaClO as oxygen source, the novel catalyst gave quantitative conversion of substrate (99%) with 40% ee value in the asymmetric epoxidation of styrene at 0 °C within 60 min (Table 1, entry 1). By contrast, only 70% conversion with 38% ee value was observed over neat complex under identical conditions (Table 1, entry 2). The remarkable enhancement of reaction rate with the employment of the **catalyst 1** might be due to the positive effect of the imidazolium-based IL linker and/or the synergistic interaction between active species and the layered GO support.^{18, 52}

To further elucidate the function of the imidazolium-based IL moiety in the water/ dichloromethane biphasic reaction, a IL-free counterpart (**catalyst 2**) was prepared as a control catalyst by directly appending the chiral salen Mn(III) complex onto amino-modified GO sheet. Interestingly, the heterogeneous **catalyst 2** offered a slightly higher TOF value than the neat complex (Table 1, entry 3 vs 2, entry 7 vs 6, entry 10 vs 9, entry 13 vs 12, entry 16 vs 15, and entry 19 vs 18). The observation clearly indicates that the layered GO support with flexible interlayer space enables the heterogeneous catalyst to behave as a pseudo-homogeneous catalyst in the epoxidation. But it does not have a great effect on boosting the reaction. Slightly higher efficiency over the **catalyst 2** is probably due to the improved mass transfer originating from the hydrophobic alkyl linker. The other control catalyst of GO-free counterpart (**IL-complex**) was also employed to confirm the little effect of GO sheets on enhancing catalytic efficiency.

Despite of similar layered structure, the IL-tagged **catalyst 1** was far more efficient than **catalyst 2** under identical reaction conditions (Table 1, entry 1 vs 3). It is logical to deduce that imidazolium-based IL moiety plays a critical role on accelerating the aqueous/organic biphasic reaction. The proximity of IL unit to the active site renders catalytic sites more accessible, thereby tuning **catalyst 1** into an efficient catalyst for this reaction.

Furthermore, the high polarity and ionic character of the IL moiety exert synergistic effect on stabilizing the active Mn^V-(salen)-oxo intermediate in the asymmetric epoxidation of unfunctionalized olefins, which in turn enhances the catalytic efficiency of chiral salen Mn(III) catalyst.

Table 1 The results of enantioselective epoxidation of unfunctionalized olefins over different chiral salen Mn(III) complexes ^a

Entry	Catalyst	Substrates	Products	Conv. ^b (%)	ee ^b (%)	Yield ^c (%)	TOF ^d ×10 ⁻³ (s ⁻¹)
1	Catalyst 1			99	40	92	6.38
2	Neat complex		 (R)	70	38	64	4.44
3	Catalyst 2			76	36	68	4.72
4	IL-complex			98	39	92	6.26
5	Catalyst 1			99	44	91	6.32
6	Neat complex		 (R)	83	43	75	5.21
7	Catalyst 2			84	42	76	5.28
8	Catalyst 1			99	73	95	6.60
9	Neat complex		 (1R, 2S)	76	72	68	4.72
10	Catalyst 2			78	72	70	4.86
11	Catalyst 1			99	84	93	6.46
12	Neat complex		 (1R, 2S)	66	80	60	4.17
13	Catalyst 2			67	80	61	4.24
14	Catalyst 1			99	92	95	6.60
15	Neat complex		 (3R, 4R)	58	94	53	3.68
16	Catalyst 2			61	95	58	4.03
17	Catalyst 1			99	93	94	6.53
18	Neat complex		 (3R, 4R)	57	95	55	3.82
19	Catalyst 2			63	95	59	4.10

^a Catalyst (4 mol% of substrate, based on Mn ion content), substrate (1 mmol), PyNO (2 mmol), NaClO (2 mmol, added in four equal parts), CH₂Cl₂ (2 mL), 60 min, 0 °C.

^b Determined by GC.

^c Isolated yields.

^d TOF is calculated by the expression of [product] / [catalyst] × time (s⁻¹).

In order to further understand the higher catalytic performance of **catalyst 1** in detail, we have used kinetics to study the reaction rates of asymmetric epoxidation of styrene over the catalysts of neat complex, **IL-complex**, **catalyst 1** and **catalyst 2**. The time-dependent plot of corresponding catalyst is shown in Fig. 8. It is observed from the profile that conversion of styrene increased linearly up to 30 min, after which a significant increase is not observed. Therefore, the initial rate constants K_{obs} were determined from the data in this time range. **Catalyst 1**, **IL-complex**, **catalyst 2** and neat complex give K_{obs} values of 2.70,

2.35, 1.81, and 1.60 M/min, respectively. The order of reaction rates over the all tested catalysts is thus as follows: **catalyst 1** > **IL-complex** > **catalyst 2** > neat complex, viewing from the kinetics point. The results demonstrated that flexible layered structure of GO sheets allowed the heterogeneous **catalysts 1** and **2** to behave as pseudo-homogeneous catalysts in the asymmetric epoxidation. Remarkable enhancement of reaction rate with the employment of **catalyst 1** should be due to the synergistic interaction between active species and layered GO support, as well as the positive effect of imidazolium-based IL linker.

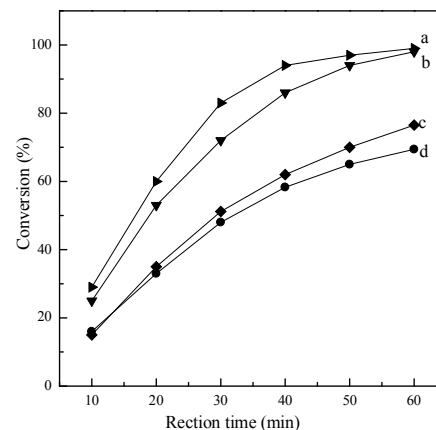


Fig. 8 The conversion vs. reaction time plot for asymmetric epoxidation of styrene catalyzed by **catalyst 1** (a), **IL-complex** (b), **catalyst 2** (c) and neat complex (d).

The positive effect of imidazolium-based IL linker on accelerating the aqueous/organic biphasic epoxidation was also observed in the case of the α -methylstyrene, indene, 1,2-dihydronaphthalene, 6-cyano-2,2-dimethylchromene, and 6-nitro-2,2-dimethylchromene, as shown by TOF values in Table 1 (Table 1, entries 5, 8, 11, 14, and 17). Notably high TOF values for **catalyst 1** were obtained with all the substrates either bulky or less, suggesting the flexible interlayer spaces of **catalyst 1** that avoided the diffusion constraint. The TOF values were significant higher than those of **catalyst 2** in the corresponding epoxidations (Table 1, entry 1 vs. 3, entry 5 vs. 7, entry 8 vs. 10, entry 11 vs. 13, entry 14 vs. 16, entry 17 vs. 19). Excellent conversions (99%) were obtained with all the alkenes used in this work but the highest asymmetric induction is observed for the electron-deficient 6-cyano-2,2-dimethylchromene (ee, 92%) and 6-nitro-2,2-dimethylchromene (ee, 93%) (Table 1, entries 14 and 17). The relatively bulkier olefins, such as indene and 1,2-dihydronaphthalene, also showed good ee values (73% and 84%, respectively) (Table 1, entries 8 and 11), while the ee values were not encouraging in the case of the terminal olefins, such as styrene and α -methylstyrene (Table 1, entries 1 and 5).

It is known that the reaction medium plays a crucial role in the catalytic performance of chiral salen Mn(III) complex in the asymmetric epoxidation of non-functionalized alkenes.^{15,37} Table 2 summarizes the results of comparative study of the enantioselective epoxidation of styrene over **catalyst 1** in various solvents. It was found that dichloromethane was the optimal solvent for the enantioselective epoxidation of styrene with NaClO, giving excellent yield of styrene epoxide with high ee value (Table 2, entry 1), whereas *n*-hexane appeared to be

unsuitable for the reaction (Table 2, entry 2). The difference should attribute to the better dispersion of **catalyst 1** in dichloromethane than in *n*-hexane. However, the catalytic performance, especially enantioselectivity of the **catalyst 1** was not encouraging in acetone, acetonitrile, and methanol, although **catalyst 1** can also be well dispersed in these media (Table 2, entries 3, 4, and 5). The principal explanation for this difference is that the solvent containing oxygen or nitrogen atom with lone electron pair can induce probably coordination with metal center of the chiral salen Mn(III) complex, suppressing the ability of the formation of the active oxygen transfer species (Mn(V)-oxo) in the epoxidation of styrene.³⁷ Furthermore, only 34% yield of styrene epoxide with 12% ee value was obtained in water, where **catalyst 1** can be readily dispersed (Table 2, entry 6). The lower activity is due to the limited solubility of styrene in the aqueous solution of catalyst and oxidant, and the poor enantioselectivity is partially due to the solvation of water.

Table 2 The results of asymmetric epoxidation of styrene in different solvent over **catalyst 1**^a

Entry	Solvent	Conv. ^b (%)	ee ^b (%)	Yield ^c (%)	TOF ^d × 10 ⁻³ (s ⁻¹)
1	dichloromethane	99	40 (R)	92	6.38
2	<i>n</i> -hexane	40	15 (R)	29	2.17
3	acetone	89	33 (R)	80	5.61
4	acetonitrile	95	30 (R)	86	6.06
5	methanol	92	27 (R)	76	5.29
6	water	57	12 (R)	34	2.52

^a **Catalyst 1** (4 mol% of substrate, based on Mn ion content), styrene (1 mmol), PyNO (2 mmol), NaClO (2 mmol, added in four equal parts), solvent (2 mL), 60 min, 0 °C.

^b Same as in Table 1.

^c Same as in Table 1.

^d Same as in Table 1.

Recycling

Although designed **catalyst 1** behaves as an efficient homogeneous catalyst, it can be facilely recovered from the aqueous/organic biphasic reaction. After the reaction, the heterogeneous **catalyst 1** was quantitatively recovered from the reaction mixture by centrifugation. The supernatant was then separated from the lower catalyst by simple decantation. The recovered catalyst was washed with ethyl acetate and dried at 40 °C overnight for reuse.

Fig. 9 shows the results of the recovery and reusability of **catalyst 1**. To our delight, **catalyst 1** could be reused for seven times with no appreciable decrease in yield and enantioselectivity of styrene epoxide. Chemical analysis of the manganese content in the supernatant revealed no detectable leaching of Mn species during the reaction. The results suggested the excellent stability and reusability of **catalyst 1** in the aqueous/organic biphasic epoxidation. UV-vis spectra gave a direct evidence of the stability of **catalyst 1** based on the fact that no significant change in the catalyst occurred even after reuse for seven times (Fig. 6b vs. b'). These observations suggested that the efficient **catalyst 1** was perfectly stable under the basic reaction condition in this work (pH 11.5, NaClO buffer), and the decomposition of chiral

salen Mn(III) complex, a main reason for deactivation of the complex under basic epoxidation conditions,⁵³ didn't occur. Short reaction time (within 60 min) and low temperature (0 °C) used in our studies should prevent or at least slow catalyst degradation. Furthermore, the imidazolium-based IL linker moiety plays a positive effect on stabilizing the complex.

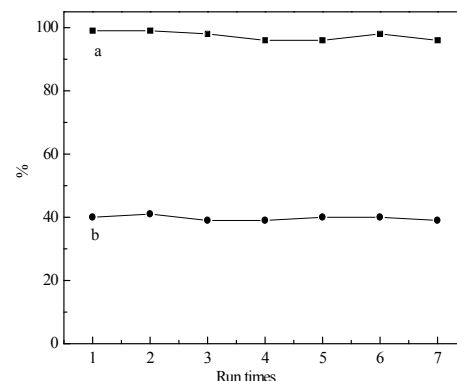


Fig. 9 Reuse of **catalyst 1** in asymmetric epoxidation of styrene with NaClO as oxidant at 0 °C (a: conversion; b: ee value).

Conclusions

The chiral Mn(III) salen complex was successfully immobilized on the flat planes and edge of the layered GO materials through an imidazolium-based IL linker. Benefiting from fascinating layered structure of the GO sheet, as well as active role of IL linker in the overall reaction mechanism, the resulting **catalyst 1** was efficient and universal in the enantioselective epoxidation of unfunctionalized olefins with aqueous NaClO as an oxidant. Remarkable enhancement of reaction rate was observed over a wide range of alkenes either bulky or less (styrene, α -methylstyrene, indene, 1,2-dihydronaphthalene, 6-cyano-2,2-dimethylchromene, and 6-nitro-2,2-dimethylchromene). Furthermore, the heterogeneous catalyst was stable in the water-CH₂Cl₂ biphasic reaction system. It could be easily recovered and recycled for seven times without significant loss of the reactivity.

Acknowledgements

The project was financial supported by the National Natural Science Foundation of China (Grant Nos. 21476069, 21003044), the Scientific Research Fund of Hunan Provincial Education Department (13B072), the Program for Excellent Talents in Hunan Normal University, the Hunan Provincial Innovation Foundation for Postgraduate (CX2013B209) and the Program for Science and Technology Innovative Research Team in Higher Educational Institutions of Hunan Province. The authors are also grateful to Dr Rongchang Luo (Sun Yat-Sen University) for his help with the characterization with XPS.

References

- 1 C. M. Clouthier and J. N. Pelletier, *Chem. Soc. Rev.*, 2012, **41**, 1585.
- 2 D. H. Paull, C. Fang, J. R. Donald, A. D. Pansick and S. F. Martin, *J. Am. Chem. Soc.*, 2012, **134**, 11128.
- 3 W. Zhang, J. L. Loebach, S. R. Wilson and E. N. Jacobsen, *J. Am. Chem. Soc.*, 1990, **112**, 2801.
- 4 S. Liao and B. List, *Angew. Chem. Int. Ed. Engl.*, 2010, **49**, 628.

- 5 H. Zhang, Y. M. Wang, L. Zhang, G. Gerritsen, H. C. Abbenhuis, R. A. van Santen and C. Li, *J. Catal.*, 2008, **256**, 226.
- 6 B. Qi, Y. Wang, L. Lou, L. Huang, Y. Yang and S. Liu, *J. Mol. Catal. A: Chem.*, 2013, **370**, 95.
- 7 R. I. Kureshy, T. Roy, N.-u. H. Khan, S. H. Abdi, A. Sadhukhan and H. C. Bajaj, *J. Catal.*, 2012, **286**, 41.
- 8 N. C. Maity, S. H. Abdi, R. I. Kureshy, N.-u. H. Khan, E. Suresh, G. P. Dangi and H. C. Bajaj, *J. Catal.*, 2011, **277**, 123.
- 9 W. Ren, X. Fu, H. Bao, R. Bai, P. Ding and B. Sui, *Catal. Commun.*, 2009, **10**, 788.
- 10 P. Barbaro and F. Liguori, *Chem. Rev.*, 2008, **109**, 515.
- 11 N. C. Maity, G. V. Rao, K. Prathap, S. H. Abdi, R. I. Kureshy, N.-u. H. Khan and H. C. Bajaj, *J. Mol. Catal. A: Chem.*, 2013, **366**, 380.
- 12 J. Huang, J. Cai, H. Feng, Z. Liu, X. Fu and Q. Miao, *Tetrahedron*, 2013, **69**, 5460.
- 13 D. Wang, M. Wang, X. Wang, R. Zhang, J. Ma and L. Sun, *J. Mol. Catal. A: Chem.*, 2007, **270**, 278.
- 14 Y. Sun and N. Tang, *J. Mol. Catal. A: Chem.*, 2006, **255**, 171.
- 15 R. Luo, R. Tan, Z. Peng, W. Zheng, Y. Kong and D. Yin, *J. Catal.*, 2012, **287**, 170.
- 16 J. Huang, X. Fu and Q. Miao, *Appl. Catal., A*, 2011, **407**, 163.
- 17 H. Shi, C. Yu and J. He, *J. Catal.*, 2010, **271**, 79.
- 18 S. He, Z. An, M. Wei, D. G. Evans and X. Duan, *Chem. Commun.*, 2013, **49**, 5912.
- 25 19 S. Stankovich, D. A. Dikin, G. H. Dommett, K. M. Kohlhaas, E. J. Zimney, E. A. Stach, R. D. Piner, S. T. Nguyen and R. S. Ruoff, *Nature*, 2006, **442**, 282.
- 20 H. Chang and H. Wu, *Adv. Funct. Mater.*, 2013, **23**, 1984.
- 21 E. Dervishi, A. R. Biris, J. A. Driver, F. Watanabe, S. Bourdo and A. S. Biris, *J. Catal.*, 2013, **299**, 307.
- 22 A. R. Siamaki, A. E. R. S. Khder, V. Abdelsayed, M. S. El-Shall and B. F. Gupton, *J. Catal.*, 2011, **279**, 1.
- 23 X. Hu, L. Mu, J. Wen and Q. Zhou, *Carbon*, 2012, **50**, 2772.
- 24 R. Tan, C. Li, J. Luo, Y. Kong, W. Zheng and D. Yin, *J. Catal.*, 2013, **298**, 138.
- 25 25 W. Zheng, R. Tan, L. Zhao, Y. Chen, C. Xiong and D. Yin, *RSC Adv.*, 2014, **4**, 11732.
- 26 X. Liu, N. Tang, W. Liu and M. Tan, *J. Mol. Catal. A*, 2004, **212**, 353.
- 27 D. Bell, M. R. Davies, G. R. Geen, I. S. Mann, *Synthesis*, 1995, **1995**, 707.
- 28 W. S. Hummers Jr and R. E. Offeman, *J. Am. Chem. Soc.*, 1958, **80**, 1339.
- 29 L. Canali, E. Cowan, H. Deleuze, C. L. Gibson and D. C. Sherrington, *J. Chem. Soc., Perkin Trans. 1.*, 2000, 2055.
- 30 30 H. M. Ren, H. Tian, H. Q. Lang, The handbook of analytical chemistry, Chemical Industry Press: Beijing, 1997; **Vol. 2**, p559.
- 31 R. I. Kureshy, I. Ahmad, N.-u. H. Khan, S. H. Abdi, K. Pathak, R. V. Jasra, *J. Catal.* 2006, **238**, 134.
- 32 Y. Liang, D. Wu, X. Feng and K. Müllen, *Adv. Mater.*, 2009, **21**, 1679.
- 33 33 S. Niyogi, E. Bekyarova, M. E. Itkis, J. L. McWilliams, M. A. Hamon and R. C. Haddon, *J. Am. Chem. Soc.*, 2006, **128**, 7720.
- 34 Y. Kong, R. Tan, L. Zhao and D. Yin, *Green Chem.*, 2013, **15**, 2422.
- 35 N. Karousis, S. P. Economopoulos, E. Sarantopoulou and N. Tagmatarchis, *Carbon*, 2010, **48**, 854.
- 36 36 C. E. Song and E. J. Roh, *Chem. Commun.*, 2000, 837.
- 37 R. Tan, D. Yin, N. Yu, Y. Jin, H. Zhao and D. Yin, *J. Catal.*, 2008, **255**, 287.
- 38 K. Smith, C. Liu and G. A. El-Hiti, *Org. Biomol. Chem.*, 2006, **4**, 917.
- 39 W. Yuan, B. Li and L. Li, *Appl. Surf. Sci.*, 2011, **257**, 10183.
- 40 40 N. V. Medhekar, A. Ramasubramaniam, R. S. Ruoff and V. B. Shenoy, *ACS Nano*, 2010, **4**, 2300.
- 41 J. Yan, G. Chen, J. Cao, W. Yang, B. Xie and M. Yang, *New Carbon Materials*, 2012, **27**, 370.
- 42 S. Stankovich, R. D. Piner, S. T. Nguyen and R. S. Ruoff, *Carbon*, 2006, **44**, 3342.
- 43 Y. Si and E. T. Samulski, *Nano Lett.*, 2008, **8**, 1679.
- 44 A. J. Patil, J. L. Vickery, T. B. Scott and S. Mann, *Adv. Mater.*, 2009, **21**, 3159.
- 45 45 M. Veerapandian, M.-H. Lee, K. Krishnamoorthy and K. Yun, *Carbon*, 2012, **50**, 4228.
- 46 S. Park, K. S. Lee, G. Bozoklu, W. Cai, S. T. Nguyen and R. S. Ruoff, *ACS nano*, 2008, **2**, 572.
- 47 G. Wang, N. Yu, L. Peng, R. Tan, H. Zhao, D. Yin, H. Qiu, Z. Fu and D. Yin, *Catal. Lett.*, 2008, **123**, 252.
- 48 48 F. Song, C. Wang, J. M. Falkowski, L. Ma and W. Lin, *J. Am. Chem. Soc.*, 2010, **132**, 15390.
- 49 X.-Z. Tang, W. Li, Z. Z. Yu, M. A. Rafiee, J. Rafiee, F. Yavari and N. Koratkar, *Carbon*, 2011, **49**, 1258.
- 50 B. Li, L. Zhou, D. Wu, H. Peng, K. Yan, Y. Zhou and Z. Liu, *ACS nano*, 2011, **5**, 5957.
- 51 K. Yu, Z. Gu, R. Ji, L. Lou, F. Ding, C. Zhang and S. Liu, *J. Catal.*, 2007, **252**, 312.
- 52 X. Li, Q. Shen, G. Zhang, D. Zhang, A. Zheng, F. Guan and Y. Sun, *Catal. Commun.*, 2013, **41**, 126.
- 53 53 X. Ma, Y. Wang, W. Wang and J. Cao, *Catal. Commun.*, 2010, **11**, 401.